This article has been accepted for publication in the Journal of Southern Hemisphere Earth Systems Science and undergone full peer review. It has not been through the copyediting, typesetting and pagination, which may lead to differences between this version and the final version.

JSHESS Accepted

DOI: 10.22499/3.6801.001

Trends and low frequency variability of East Coast Lows in the twentieth century

Fei Ji [1], Acacia S. Pepler [2], Stuart Browning[3], Jason P. Evans[2], Alejandro Di Luca[2]

[1] New South Wales Office of Environment and Heritage, Sydney, Australia

[2] Centre of Excellence for Climate System Science and Climate Change Research Centre, University of New South Wales, Sydney, Australia

[3] Department of Environmental Sciences, Macquarie University, Sydney, Australia

Abstract

East Coast Lows (ECLs) are important weather systems that affect the eastern seaboard of Australia. They have attracted research interest for both their destructive nature and water supplying capability. In this paper, three objective ECL tracking methods are applied to the twentieth century reanalysis ensemble (20CR V2C) for the period of 1851–2014 to identify historical trends and variability in ECLs. While the ensemble mean is unsuitable for tracking ECLs, when all methods are applied to the full 56-member ensemble there is large agreement between tracking methods as to the low-frequency variability and trends in ECLs. The uncertainty between 56 ensemble members has dramatically decreased in recent decades. For comparison, the three tracking methods are also applied to ERA-I reanalysis dataset for the overlapping time period (1980-2009). The inter-annual variability and monthly distribution of ECLs agrees well between different reanalysis for each of tracking methods. The most recent decade has had relatively low numbers of ECLs compared to the previous century.

1. Introduction

East Coast Lows (ECLs) are intense low-pressure systems that occur several times each year off the eastern coast of Australia, in particular southern Queensland, New South Wales (NSW), and in eastern Victoria (Hopkins and Holland, 1997). ECLs are most common in winter (June-August) with a maximum frequency in June, although they can occur in any season. ECLs are one of the main influences on rainfall variability and severe weather in this region (e.g. Dowdy et al. 2014, Callaghan & Power, 2014, Kiem et al 2016).

ECLs often intensify rapidly overnight making them one of the most dangerous weather systems to affect the Australian eastern coast (Holland et al 1987). They can generate heavy widespread rainfall leading to flash and/or major river-flooding, gale or storm force winds along the coast and adjacent waters, and very rough seas and prolonged heavy swells over coastal and ocean waters which can cause damage to the coastline (e.g. Abbs, et al 2006; Callaghan and Helman, 2008; Speer et al., 2009; Dowdy et al., 2014). The falling trees and flash flooding have caused fatalities on the land and large vessels have run aground during these events. For example, an ECL on 8th of June 2007 caused extensive damage along the central NSW coastline including the beaching of the bulk carrier 'Pasha Bulker', nine deaths, major flash flooding, extreme wind gusts and sea waves, and over $1.5 billion in damage (Verdon-Kidd et al 2010, 2016; Mills et al 2010). Although ECLs can cause significant damage to coastal infrastructure and ecosystems, they also contribute positively to the fresh water resources in eastern Australia, particularly in north-eastern NSW (Risbey et al. 2009a, Pepler and Rakich 2010, Pepler et al. 2014).

Historically, ECLs have mainly been investigated in the context of individual or a group of events (Bridgman 1985; Holland et al. 1987; McInnes et al. 1992; Hopkins and Holland 1997, Leslie and Speer 1998, Qi et al. 2006; Mills et al. 2010; Verdon-Kidd et al 2010; Evans et al 2012; Ji et al. 2011, 2014, Gilmore et al. 2015, Pepler et al 2016c). There has been some effort to build ECL datasets using various classification schemes based on surface variables, but these have generally been for periods shorter than

50 years (PWD 1985, 1986; Holland et al. 1987; Hopkins and Holland 1997; Qi et al. 2006, Speer et al 2009, 2011).

In more recent years, several objective tracking schemes (Pepler and Coutts-Smith 2013; Browning and Goodwin 2013) and a detection scheme (Dowdy et al. 2013) have been widely used in detecting ECLs in Australia. These use a range of approaches, resulting in clear differences in observed ECL seasonality and inter-annual variability, although all show similar skill at identifying the most significant and impactful events (Pepler et al. 2015). The different methods also give a range of future trends when applied to regional climate model data, with the uncertainty related to the choice of identification method similar in magnitude to the uncertainty between different sets of climate models (Ji et al. 2015, Pepler et al. 2016a).

To understand future changes in ECL activity, it is important to first understand how cyclones have changed over the past century. While this has been performed manually for the subset of ECLs associated with severe coastal flooding (Power and Callaghan 2015), this task is too arduous to be completed manually for the full range of ECLs. Instead, long datasets of ECLs using automated methods have recently become possible using long reanalysis datasets such as the 20th Century Reanalysis (20CR v2c; Compo et al. 2011). This has been used to identify trends and variability in historical ECLs using two different approaches (Pepler et al. 2016b, Browning and Goodwin 2016), both of which identify a step-change in agreement between ensemble members in the mid-1950s, with additional uncertainty prior to the mid-1910s.

However, as the identification of cyclones is sensitive to the method used to identify the cyclones, several questions remain. Are the multi-decadal variability and observed trends in ECL frequency consistent across all methods used to identify ECLs, and can these be related to major climate drivers? How sensitive are different methods to the increasing uncertainty in the reanalysis ensemble prior to the 1950s? What are the true trends in ECL frequency over the twentieth century?

In this study, we apply the three objective tracking methods (Pepler and Coutts-Smith 2013, Browning and Goodwin 2013 and Dowdy et al. 2011) to the 20CR reanalysis data to explore the long-term variation of ECLs, and compare the similarity and differences in tracking ECLs.

2. Data

The data used in this study are global 6-hourly MSLP and geopotential at 500hpa fields from the 56-member 20CR V2C ensemble and the ensemble-mean analyses spanning the 164-year period from 1851 to 2014 (NOAA, 2016). 20CR V2C uses the same model as 20CR version 2 (Compo et al. 2011) with new sea ice boundary conditions from the COBE-SST2, new pentad Simple Ocean Data Assimilation with sparse input (SODAsi.2) sea surface temperature fields, and additional observations.

The analyses are generated by assimilating only surface pressures and using monthly sea surface temperature (SST) and sea ice distributions as boundary conditions within a 'deterministic' Ensemble Kalman Filter (EKF). A unique feature of the 20CR is that estimates of uncertainty are derived using a 56 member ensemble. Overall, the quality is approximately that of current three-day Numerical weather prediction (NWP) forecasts. The NWP model used is the NCEP Global Forecast System, a coupled atmosphere-land model, at a T62 (approximately 1.9 degree) horizontal resolution with 28 vertical hybrid sigma-pressure levels (Compo et al. 2011).

A more modern reanalysis, ERA-Interim (Dee et al. 2011), is also used to evaluate the 20CR reanalysis during the recent period 1980 to 2009. The spatial resolution of ERA-Interim is 0.75x0.75 degrees which is finer than 20CR with resolution of 2x2 degrees. Di Luca (2015) showed that fewer ECLs are identified on average using lower resolution reanalyses, hence we expect 20CR to have fewer ECLs than ERA-Interim just due to this effect.

The subjectively analysed ECL database (Speer et al 2009), which is referred to as the Maritime Low Database (MLD), is the available “subjectively analysed dataset” to evaluate objective tracking results. The dataset was constructed from daily charts of mean sea level pressure, station data and satellite images, includes details (date, intensity, and category etc.) for each ECL event in the region indicated in Figure 1 between 1970 and 2006, as identified through manual inspection of the 0000UTC synoptic

charts. This database averages 22 ECLs per year, many of which have no identified weather impacts on the Australian coast.

Some major climate drivers including El Niño–Southern Oscillation (ENSO), the Indian Ocean Dipole (IOD), the Southern Annular Mode (SAM; Risbey et al. 2009b), the Interdecadal Pacific Oscillation (Folland et al. 2002) are used to discuss the large scale climate modes influence on ECLs. In this study the oceanic component of canonical ENSO is represented by the Niño 3.4 SST anomaly (SSTa) index calculated using the definition of Trenberth (1997). NINO3.4 is used since this has been shown to be more closely related to Australian climate than NINO3 (Wang and Hendon, 2007). To represent non-canonical central Pacific ENSO we use the ENSO Modoki index calculated using the definition of Ashok et al. (2007). The Southern Oscillation Index (SOI; atmospheric component of ENSO) is calculated as the normalised sea level pressure difference between Tahiti and Darwin. To represent Pacific decadal variability, we use the IPO index calculated using the tripole approach of Henley et al (2015) as the tripole index is a simple but robust index of IPO which has become widely used for studies of interdecadal variability, particularly in Australia.

SOI, IPO, and Nino3.4 indices are downloaded from http://www.esrl.noaa.gov/psd/data/climateindices/list/, SAM can be found at http://www.nerc-bas.ac.uk/icd/gjma/sam.html (Marshall, 2003), ENSO Modoki and IOD are from http://www.jamstec.go.jp/frsgc/research/d1/iod/modoki_home.html.en, and http://www.jamstec.go.jp/frcgc/research/d1/iod/DATA/dmi.monthly.txt , respectively.

3. Method

The three objective tracking methods are described in Pepler and Coutts-Smith (2013), Browning and Goodwin (2013), and Dowdy et al. (2011). They are further summarized in Pepler et al (2015). Each of the low tracking methods has some tunable parameters, which can result in large variability in the numbers of ECLs identified. In this paper, our purpose is to compare long term trend and low frequency variability of ECLs between different methods, therefore, we do not restrict each method to identify

similar number of ECLs. The normalized ECL distribution instead of actual distribution of annual and monthly ECLs is used for the comparisons.

The Pepler and Coutts-Smith (2013) method is based on the University of Melbourne cyclone tracking scheme (Murray and Simmonds 1991, Simmonds et al. 1999), and is referred to as the Laplacian method (LAP). This method first identifies a maximum in the Laplacian of sea level pressure, before employing an iterative technique to identify a corresponding pressure minimum from a spline-fitted pressure field and joining cyclones into a single event track. To be considered an ECL, a cyclone must have an average intensity (Laplacian) within 2° of the cyclone center greater than 1 hPa.(deg lat)$^{-2}$, persist for at least two instances (6 hours), and be within the ECL region marked in Figure 1 in at least one instance. These criteria were chosen to give a frequency of 22 ECLs p.a. using the ERA-Interim reanalysis, consistent with the subjective ECL database.

The Browning and Goodwin (2013; 2016) approach uses the average pressure gradient to decide on the existence of a cyclone and to indicate the intensity of the cyclone, similar to Alpert (1990), this approach is referred to as the Pressure Gradient (PG) method. In the PG method, closed low pressure systems are identified from un-interpolated sea level pressure fields within the region shown in Figure 1. A low is declared when the pressure gradients between all eight surrounding cells and the central cell are positive, and the average of these pressure gradients exceeds 1hPa. These lows are then grouped into events based on their geographical proximity. Additional criteria are imposed to restrict the dataset to only events likely to have impacted the coastline: events are required to have a minimum duration of 18 hours; events must, at some stage, achieve a pressure gradient of least 6 hPa per 4° (latitude–longitude) (~350 km); and this pressure gradient must be oriented such that the inferred geostrophic wind field is directed toward the coast. These criteria differ from those used in Di Luca et al. (2015) and Pepler et al. (2015), and are described in more detail in Browning and Goodwin (2013; 2016).

Dowdy et al (2011, 2013a) attempted to identify ECL favorable conditions in the upper level circulation, which are easier to apply to global climate models than methods that identify individual surface lows (Dowdy et al. 2013b, 2014). This method is referred to as the upper level geostrophic vorticity approach (ULGV), and uses the maxima of 500 hPa geostrophic vorticity in a region to the northwest of the main

ECL area for each 6-hourly observation to identify periods where the likelihood of ECL formation is enhanced. While all ECL tracking methods are sensitive to the resolution of the reanalysis used (Di Luca et al. 2016), this approach is particularly sensitive to changes in the climatology of ULGV between reanalyses. Consequently, this method uses different intensity thresholds for each reanalysis and ensemble member. ULGV adjusts thresholds for each of 56 members to match number of identified ECLs for 1970 to 2006 to 22 ECLs per year, approximating the numbers observed in the MLD, this is similar to the approach used for ECLs in Dowdy et al. (2011, 2013), as well as for front identification schemes in other studies (e.g. Hope et al. 2013). The thresholds of ULGV are slightly different between the 56 ensemble members varying from the 86th to 88th percentile of maximum GV from 1850 to 2014, however the threshold of duration is same (at least 12 hours) for all ensemble members.

The 20CR ensemble mean has consistently been demonstrated to have large step changes in cyclone frequency related to changes in data availability, particularly for the southern hemisphere, and cannot be used prior to the mid-1950s (Wang et al. 2013, Pepler et al. 2016b, Browning and Goodwin 2016). Unless otherwise noted, in this paper "ensemble mean" refers to the average ECL frequency across the 56 ensemble members, with each member equally weighted, which is a much better indication of the true ECL frequency. In the limit of large ensembles, the error in the ensemble mean is, on average, half of that for a randomly drawn ensemble member (Holton, et al, 2013).

The ensemble mean is normalized to compare the annual and monthly ECLs indicated by the three methods (LAP, PG, and ULGV) and using two different reanalysis datasets (20CR and ERA-I). The formula $(X - \bar{X})/\bar{X}$ is used to normalize variable x, where $\bar{X}$ is mean of X.

The formula 100 x (max number of tracked ECLs – minimum number of tracked ECLs)/(ensemble mean) is used to quantify relative uncertainty range for each of the three methods (LAP, PG, and ULGV).

We also analyze changes in the frequency of the strong ECLs for each of the methods. The threshold of 2 hPa.(deg lat)$^{-2}$ is used for the LAP method and 8 hPa per 4° (latitude–longitude) (~350 km) for the PG method to extract the strong ECLs. A different method is used for the ULGV method. The threshold

is adjusted to have about 5 strong ECLs a year for 1970-2006, then the threshold is applied for the whole time period (1851-2014) to have strong ECLs time series.

The Pearson's correlation is calculated to assess the teleconnection of ECL frequency with major climate drivers. The time period of climate drivers is 1950-2014 for Nino3.4, 1951-2014 for SOI, 1957-2014 for SAM, 1870-2014 for IOD, and 1870-2014 for IPO and ENSO Modoki. We note that as SST data were sparse in the early period, these indices have considerably more uncertainty then. The correlation is calculated for the overlap period (1957-2014) and for the whole time period.

In this study, we first compare the identified ECLs between 20CR and ERA-In, and between 20CR and the MLD dataset to assess the three method's capability to identify ECLs. Then we investigate long term trends and low frequency variability of ECLs, and the monthly distribution and possible seasonal shift of ECLs. We then investigate relationships between large scale climate drivers and ECLs. Finally, we analyze the variation of uncertainty range for indicated ECLs.

4. Results

4.1 Evaluation of identified ECLs

During the overlap period, 1980-2009, all three tracking schemes have interannual correlations greater than 0.7 ($n=30$, $p>0.01$) between the number of ECLs in the ERA-Interim reanalysis and the average frequency of ECLs across the 56 members of the 20CR ensemble (Fig 2), with very similar monthly distributions of ECL frequency (correlations above 0.9 for all methods) (Fig 3). However, while the ULGV method by design has the same average ECL frequency in both the 20CR and ERA-Interim reanalysis, the average frequency of ECLs in the 20CR is lower than ERAI for both the LAP and PG methods, a decline of 16% and 28% respectively. This was also observed in Pepler et al. (2016), and could be related to the lower spatial resolution, which has been shown to influence the frequency of cyclones identified for a given intensity threshold (e.g. Di Luca et al. 2015).

Due to the different annual ECL frequencies for the different tracking schemes, annual frequencies have been normalized so that they have the same average frequency during the period 1970-2006. During this period, the inter-annual correlations between ECLs using the three subjective methods range

between 0.65 and 0.78 (Fig 4), similar to the correlations reported in Pepler et al. (2015), with slightly lower correlations (0.54-0.57) between each method and the subjective MLD ECLs. Interestingly, while there is no trend in the MLD during this period, all tracking schemes identify a weakly declining ECL frequency in the 20CR reanalysis during this period even if these trends are not significant.

Normalized monthly ECLs for the three tracking schemes and the MLD are shown in Fig 5. All three tracking methods indicate that ECLs are most common in the winter (JJA), which is the same as that observed in the MLD. The distribution of monthly ECLs for LAP and PG are the most similar to that in MLD, with correlations around 0.88. However, ULGV indicated more ECLs in cold months and fewer ECLs in warm months than LAP, PG and MLD, which was also observed in Pepler et al. (2015). LAP and PG both indicated the maximum ECLs in September, which is consistent with MLD, but the ECL peak indicated by ULGV is in August.

4.2 Low frequency variability and trend

The long-term normalized annual ECLs using the three methods are summarized in the Figure 6. During the period where the 20CR is relatively well constrained by surface observations, 1961-2014, the inter-annual correlations between the three methods are between 0.57 and 0.72, similar to the ERA-Interim reanalysis (Pepler et al. 2015). However, these correlations strengthen during the full 1871-2014 period, with a very strong correlation (0.87) between annual frequency using LAP and PG on the 20CR data. The low frequency variability of ULGV is similar to that of LAP and PG, especially for the period of 1890-1950, the correlations are 0.74 and 0.73 with LAP and PG respectively.

The stronger inter-annual correlations in earlier periods may reflect stronger agreement on multi-decadal variability/trends than on shorter timescales. However, it is also influenced by the shared sensitivity to decreasing data quality prior to the 1950s, particularly during the late 19th century (e.g. Wang et al. 2013, Pepler et al. 2016b). ULGV is found to be much more sensitive to changing reanalysis quality than the MSLP-based datasets, with a much stronger decline in ECL frequency prior to the 1950s (Figure 6). The higher sensitivity of the ULGV method to changes in data quality is unsurprising,

as the 20CR is only constrained by surface observations, so there is larger uncertainty in the upper atmosphere.

The decrease in ECL frequency in the late 19th is true in all seasons, but particularly during the summer months (Figure S1-S4). This may reflect the tendency for cyclones in this season to be weaker and smaller, with the skill at identifying these cyclones in reanalysis products lower even in recent decades (Pepler et al. 2015).

A clear increasing trend of ECLs can be observed for all three methods between 1880 and 1920, with a similar increasing rate, as the reanalysis becomes more reliable. There is no trend during 1920-1975 for LAP and PG, but a clear increasing trend for ULGV. In contrast, a clear decreasing trend of ECLs can be witnessed between 1975 and 2014. This indicates that a similar trend and low frequency variability can be observed in each of the three tracking method results, which is consistent with cyclone activity index described in Wang et al. (2013) for South Hemisphere.

The normalized strong ECLs for three methods are presented in the Figure S5. It is clear that inter-annual variability for the strong ECLs are much larger than that for all ECLs. Generally there is an increasing trend in the number of strong ECLs before 1960s, and there is not much change afterwards. Similar to all ECLs, the ULGV gives a larger trend than other two methods. The ratio of strong events shows increasing trend for all three methods, the ratio is higher in recent 50 years than earlier periods for each method (Figure 7), however the mean ratio doesn't show any trend within the recent decades.

4.3 Monthly distribution and seasonal shift

Long-term normalized monthly ECLs for 1851-2014 is similar to that for 1970-2006 for each method (Figure 8). Cold months dominant ECLs can be observed in all results. ULGV has a larger seasonal cycle than LAP and PG with more ECLs in the cold months and fewer in warm months. However, a clear decrease of ECL frequency in early winter and an increase in late winter/early spring (SON) can be observed in each result. The peak of monthly ECLs for 1851-2014 was shifted from early winter to late winter and early spring for 1970-2006, which is consistent in all results. This seasonal shift of monthly ECLs can be also observed in the two most recent 30-year periods as well (Fig S6).

We further analyse changes in seasonal ECLs for two specific periods (increasing in annual ECL frequency for 1895-1954, and decreasing in annual ECL frequency for 1955-2014). During the first period, an increase in annual ECL frequency mostly occurs in spring and autumn (Figure 9), however, the decrease in annual ECL frequency mostly occurs in winter for the second time period (Figure 10). This winter decline is also observed in future projections of ECLs (Ji et al, 2015, Pepler et al 2016b).

4.4 Teleconnection with major climate drivers

The relationships between ECL frequency and major climate drivers are moderate to weak for both annual and cold season (May-Sept) means (Table 1), regardless of the ECL identification method used. ECL frequency has almost no correlation with SAM. Negative correlation is observed between ECL frequency and other major climate drivers except for SOI. ECLs are favoured during La Niña periods, with a weakly positive correlation between ECL frequency and the SOI for all indices, and weakly negative correlations with NINO3.4 and ENSO Modoki. This has previously been identified for ECLs associated with major flooding on the east coast (Power and Callaghan 2016) and the PG method (Browning and Goodwin 2013), and may be related to the generally lower surface pressures recorded over northern and eastern Australia during La Niña years. Weakly negative correlations are also observed between ECL frequency and both the IPO and IOD. The correlation between ECL frequency and climate drivers are generally weak, this indicates that ECLs are a regional low system which are not strongly influenced by the major climate drivers that affect rain elsewhere in southeast Australia.

4.5 Uncertainty

The 20CR data has known temporal inhomogeneities, especially in the early decades in which the uncertainty (i.e., inter-member variability) is much larger due to the much lower number and spatial density of observations available for assimilation (Wang et al. 2013). The relative uncertainty ranges (between maximum and minimum number, and between 75^{th} and 25^{th} percentile of the number) of ECLs for the 56 ensemble members are summarized in Figure 11. Larger uncertainty in early decades and much less uncertainty in recent decades are observed in the results using the three tracking methods. In early decades, the uncertainty can be larger than 100%, relative to ensemble mean, however, the

uncertainty ranges reduce to 40-50% in recent decades. The linear decreasing trend in ensemble uncertainty can be generally observed in all results.

The relative uncertainty range for PG indicated ECLs shown in Fig 11 tends to be larger than that for LAP and ULGV indicated ECLs. This is possibly due to larger threshold values used in the analyses that results in a smaller number of mean indicated ECLs. For the similar range of differences in 56 ensemble members, the relative uncertainty range is larger, the ULGV method does show smaller uncertainty when comparing with the LAP method as they indicate a similar number of ECLs.

5. Conclusion

In this study, three objective ECL tracking methods (LAP, PG and ULGV) are applied to twentieth century reanalysis (20CR) 6-hourly mean sea level pressure and geopotential at 500hpa fields for the period 1851–2014 to infer historical trends and variability in ECLs.

The results using three tracking methods are firstly evaluated against the ERA-Interim reanalysis (1980-2009) and a subjective database of ECLs (MLD). All three results fully capture the inter-annual variability of ECLs for this period, the weak decreasing trend in ECL number, and winter dominant ECL distribution. However, both the LAP and PG methods identify fewer ECLs using the 20CR than the ERA-Interim reanalysis, which is likely related to the lower spatial resolution of 20CR (see Di Luca et al 2015). The differences in monthly ECLs between reanalyses are generally smaller than the differences between different tracking methods.

The tracking methods are applied to each of the 56 ensemble members individually, ECL statistics for three tracking methods obtained by averaging statistics from individual members generally agree well. A clear increasing trend of annual ECL frequency can be observed for all three methods between 1880 and 1920, with a similar increasing rate. There is no trend between 1920 and 1975 for LAP and PG even through there is an increase in the availability of surface observation. This indicates the density of surface observation may have less of an effect on estimated ECL numbers than is implied. The ULGV method is particularly sensitive to the quality of the 20CR reanalysis compared to other two methods. In contrast, a clear decreasing trend in annual ECL frequency can be seen between 1975 and 2014 with

a similar decreasing rate. During the late18th century and early 19th century, the increase in annual ECL frequency is mostly contributed by spring and autumn ECLs, however the decrease in ECL frequency during recent decades is mostly caused by a decrease in winter ECLs. A seasonal shift of monthly ECLs from early winter to late winter/early spring is consistent in all three tracking methods for 1970-2006 relative to 1851-2014 and for the two most recent 30-year periods.

The relationships between ECL frequency and major climate drivers are moderate to weak. Negative phase of climate major climate drivers such as Nino 3.4, Modoki, IPO, and IOD are favorable conditions for low systems except for SOI that is opposite to other drivers and SAM that has no relation to ECLs. The uncertainty between 56 ensemble members has been dramatically decreased in the recent decades for all methods.

In summary, ECLs statistics for three tracking methods obtained by averaging statistics from individual members generally agree well with similar low frequency variability and seasonal shift of ECLs, although as with previous studies this variability has little relationship with the main climate drivers. The inter-annual variability and monthly distribution of ECLs agree well between different reanalysis for each of the tracking methods, with a decline in winter ECL frequency over the last 60 years. This is consistent with future projections of ECL activity (e.g. Ji et al. 2015, Pepler et al. 2016a).

Acknowledgement

This work is made possible by funding from the NSW Environmental Trust for the ESCCI-ECL project, the NSW Office of Environment and Heritage backed NSW/ACT Regional Climate Modelling Project (NARCliM), and the Australian Research Council as part of the Future Fellowship FT110100576 and Linkage Project LP120200777. The modelling work was undertaken on the NCI high performance computers in Canberra, Australia, which is supported by the Australian Commonwealth Government.

Support for the Twentieth Century Reanalysis Project dataset is provided by the U.S. Department of Energy, Office of Science Innovative and Novel Computational Impact on Theory and Experiment (DOE INCITE) program, and Office of Biological and Environmental Research (BER), and by the National Oceanic and Atmospheric Administration Climate Program Office."

References

Abbs, D., Aryal, S., Campbell, E., McGregor, A., Nguyen, K., Palmer, M., Rafter, A., Watterson, I., and Bates, B. 2006. Projections of Extreme Rainfall and Cyclones: Final Report to the Australian Greenhouse Office. CSIRO Marine and Atmospheric Research, Aspendale, Victoria.

Alpert, P., Neeman, B.U. and Shay-El, Y. 1990. Climatological analysis of Mediterranean cyclones using ECMWF data. Tellus A, 42, 65–77. doi:10.1034/j.1600-0870.1990.00007.x

Bridgman, H. 1985. The Sygna storm at Newcastle – 12 years later. Meteorology Australia, VBP 4574, 10–16

Ashok, K., Behera, S.K., Rao, S.A., Weng, H. and Yamagata, T. 2007. El Niño Modoki and its possible teleconnection. J. Geophys. Res., 112, C11007, doi:10.1029/2006JC003798.

Browning, S.A. and Goodwin, I. 2013. Large Scale Influences on the Evolution of Winter Subtropical Maritime Cyclones Affecting Australia's East Coast. Mon Wea Rev. 41:2416-2431, doi:10.1175/MWR-D-12-00312.1.

Browning, S.A. and Goodwin, I. 2016. Large-scale drivers of Australian East Coast Cyclones since 1851, Journal of Southern Hemisphere Earth Systems Science (2016) 66: 146–171

Callaghan, J. and Helman, P. 2008. Severe Storms on the East Coast of Australia, 1770-2008. Griffith Centre for Coastal Management. Griffith University: Gold Coast, QLD, Australia.

Callaghan, J. and Power, S.B. 2014: Major coastal flooding in southeastern Australia 1860–2012, associated deaths and weather systems. *Austr Meteorol Oceanogr J*. 64, 183–213

Compo, G.P., Whitaker, J.S., Sardeshmukh, P.D., Matsui, N., Allan, R.J., Yin, X., Gleason, B.E., Vose, R.S., Rutledge, G., Bessemoulin, P., Brönnimann, S., Brunet, M., Crouthamel, R.I., Grant, A.N., Groisman, P.Y., Jones, P.D., Kruk, M.C., Kruger, A.C., Marshall, G.J., Maugeri, M., Mok, H.Y., Nordli, Ø., Ross, T.F., Trigo, R.M., Wang, X.L., Woodruff, S.D. and Worley, S.J. 2011. The Twentieth Century Reanalysis project. Q. J. R. Meteorol. Soc. 137: 1–28, doi: 10.1002/qj.776.

Dee, D.P., Uppala, S.M., Simmons, A.J., Berrisford, P., Poli, P., Kobayashi, S., Andrae, U., Balmaseda, M.A., Balsamo, G., Bauer, P., Bechtold, P., Beljaars, A.C.M., van de Berg, L., Bidlot, J., Bormann, N., Delsol, C., Dragani, R., Fuentes, M., Geer, A.J., Haimberger, L., Healy, S.B., Hersbach, H., Hólm, E.V., Isaksen, L., Kållberg, P., Köhler, M., Matricardi, M., McNally, A.P., Monge-Sanz, B.M., Morcrette, J-J., Park, B-K., Peubey, C., de Rosnay, P., Tavolato, C., Thépaut, J-N. and Vitart, F. 2011. The ERA-Interim reanalysis: configuration and performance of the data assimilation system. Q. J. R. Meteorol. Soc. 137: 553–597, doi: 10.1002/qj.828.

Dowdy, A.J., Mills, G.A. and Timbal, B. 2011. Large-scale indicators of Australian East Coast Lows and associated extreme weather events. CAWCR Technical Report 37

Dowdy, A.J., Mills, G.A. and Timbal, B. 2013a. Large-scale diagnostics of extratropical cyclogenesis in eastern Australia , Int J Climatol 33(10), 2318-2327. DOI: 10.1002/joc.3599

Dowdy, A.J., Mills, G.A., Timbal, B. and Wang, Y. 2013b. Changes in the risk of extratropical cyclones in eastern Australia. J Clim 26(4), 1403-1417, doi:10.1175/JCLI-D-12-00192.1

Dowdy, A.J., Mills, G.A., Timbal, B. and Wang, Y. 2014. Fewer large waves for eastern Australia due to decreasing storminess. Nature Climate Change, doi: 10.1038/NCLIMATE2142, 283-286.

Di Luca, A., Evans, J.P., Pepler, A., Alexander, L. and Argüeso, D. 2015. Resolution sensitivity of cyclone climatology over eastern Australia using six reanalysis products. J. Clim. 28: 9530–9549, doi: 10.1175/JCLI-D-14-00645.1.

Evans, J.P., Ekstrom, M. and Ji, F. 2012. Evaluating the performance of a WRF physics ensemble over South-East Australia, Clim Dyn, 39:1241–1258, DOI 10.1007/s00382-011-1244-5

Evans, J.P., Ji, F., Lee, C., Smith, P., Argüeso, D. and Fita, L. 2014. Design of a regional climate modelling projection ensemble experiment – NARCliM, Geosci Model Dev 7(2), 621-629, doi: 10.5194/gmd-7-621-2014

Folland, C.K., Renwick, J.A., Salinger, M.J. and Mullan, A.B. 2002. Relative influences of the Interdecadal Pacific Oscillation and ENSO on the South Pacific Convergence Zone. *Geophys. Res. Lett*, 29, 1643, doi:10.1029/2001GL014201.

Gilmore, J.B., Evans, J. P., Sherwood, S. C., Ekstrom, M. and Ji F. 2015. Extreme Precipitation in WRF during the Newcastle East Coast Low of 2007, Theoretical and Applied Climatology, accepted on June 30, 2015.

Henley, B.J., Gergis, J., Karoly, D.J., Power, S., Kennedy, J. and Folland, C.K. 2015. A Tripole Index for the Interdecadal Pacific Oscillation. *Clim. Dynam*, doi:10.1007/s00382-015-2525-1.

Holland, G.J., Lynch, A.H., and Leslie, L.M. 1987. Australian East-Coast Cyclones. Part I: Synoptic Overview and Case Study. J Clim 115, 3024–3036.

Holton, J.R. and Hakim, G.J. 2013. A introduction to dynamic meteorology (Fifth Edition). Page 532. Academic Press.

Hopkin, L.C. and Holland, G.J. 1997. Australian heavy-rain days and associated east coast cyclones: 1958-92. J Clim 10, 621–635, doi: 10.1175/1520-0442(1997)010<0621:AHRDAA>2.0.CO;2.

Ji, F., Evans, J.P. and Ekstrom, M. 2011. Using dynamical downscaling to simulation rainfall for East Coast Low events. In Chan, F., Marinova, D. and Anderssen, R.S. (eds) MODSIM2011, 19th International Congress on Modelling and Simulation. Modelling and Simulation Society of Australia and New Zealand, December 2011, pp. 1652-1658. ISBN: 978-0-9872143-1-7. www.mssanz.org.au/modsim2011/F5/ji.pdf

Ji, F., Ekstrom, M., Evans, J.P. and Teng, J. 2014. Evaluating rainfall patterns using physics scheme ensembles from a regional atmospheric model, Theoretical and Applied Climatology, 115:297-304, DOI: 10.1007/s00704-013-0904-2

Ji, F., Evans, J.P., Argüeso, D., Fita, L. and Di Luca, A. 2015. Using large-scale diagnostic quantities to investigate change in East Coast Lows, Climate Dynamics, 1–11. http://doi.org/10.1007/s00382-015-2481-9

Kalnay, E., Kanamitsu, M., Kistler, R., Collins, W., Deaven, D., Gandin, L., Iredell, M., Saha, S., White, G., Woollen, J., Zhu, Y., Leetmaa, A., Reynolds, R., Chelliah, M., Ebisuzaki, W., Higgins, W., Janowiak, J., Mo, K.C., Ropelewski, C., Wang, J., Jenne, R. and Joseph, D. 1996: The NCEP/NCAR

40-Year Reanalysis Project. Bull. Amer. Meteor. Soc., 77, 437–471. doi:10.1175/1520-0477(1996)077<0437:TNYRP>2.0.CO;2

Kiem, A.S., Twomey, C., Lockart, N., Willgoose, G., Kuczera, G. and Chowdhury, A. et al. 2016. Links between East Coast Lows and the spatial and temporal variability of rainfall along the eastern seaboard of Australia, Journal of Southern Hemisphere Earth System Science, 66 162-176

Leslie, L.M. and Speer, M.S. 1998. Short-range ensemble forecasting of explosive Australian east coast cyclogenesis, Weather and Forecasting, 13(3), 822-832, **DOI:** 10.1175/1520-0434(1998)013<0822:SREFOE>2.0.CO;2

Marshall, G.J. 2003. Trends in the Southern Annular Mode from observations and reanalyses. *J. Clim.,* **16,** 4134-4143

McInnes, K., Leslie, L. and McBride, J. 1992. Numerical simulation of cut-off lows on the Australian east coast: Sensitivity to sea-surface temperature. Int J Climatol 12, 783–795.

Mills, G.A., Webb, R., Davidson, N., Kepert, J., Seed, A. and Abbs, D. 2010. The Pasha Bulker east coast low of 8 June 2007. CAWCR Technical Report No. 23. Centre for Australian Weather & Climate Research, Melbourne, Australia.

Murray, R.J. and Simmonds, I. 1991. A numerical scheme for tracking cyclone centres from digital data. Part I: development and operation of the scheme. Aust. Meteorol. Mag. 39: 155–166.

National Center for Atmospheric Research Staff (Eds). Last modified 02 Mar 2016. "The Climate Data Guide: NOAA 20th-Century Reanalysis, Version 2 and 2c." Retrieved from https://climatedataguide.ucar.edu/climate-data/noaa-20th-century-reanalysis-version-2-and-2c. - See more at: https://climatedataguide.ucar.edu/climate-data/noaa-20th-century-reanalysis-version-2-and-2c#sthash.L8BD1Fis.dpuf

Pepler, A**.** and Rakich, C. 2010. Extreme inflow events and synoptic forcing in Sydney catchments. *IOP Conf. Ser.: Earth Environ. Sci.* 11 012010.

Pepler, A.S. and Coutts-Smith, A. 2013. A new, objective, database of east coast lows. Aust. Meteorol. Oceanogr. J. 63: 461–472.

Pepler, A., Coutts-Smith, A. and Timbal, B. 2014. The role of East Coast Lows on rainfall patterns and inter-annual variability across the East Coast of Australia. *Int. J. Climatol*., 34: 1011–1021. doi: 10.1002/joc.3741

Pepler, A.S., Di Luca, A., Ji, F., Alexander, L.V., Evans, J.P. and Sherwood, S.C. 2015. Impact of identification method on the inferred characteristics and variability of Australian east coast lows. Mon. Weather Rev. 143: 864–877, doi: 10.1175/MWR-D-14-00188.1.

Pepler A.S., Di Luca, A., Ji, F., Alexander, L.V., Evans, J.P. and Sherwood, S.C. 2016a. Projected changes in east Australian midlatitude cyclones during the 21st century, Geophysics Research Letters, Vol 43(1), 334-340, doi:10.1002/2015GL067267

Pepler, A.S., Fong, J. and Alexander, L.V. 2016b. Australian east coast mid-latitude cyclones in the 20th Century Reanalysis ensemble, Int. J. Climatol., Published online in Wiley Online Library, DOI: 10.1002/joc.4812

Pepler, A.S., Alexander, L.V., Evans, J.P. and Sherwood, S.C. 2016c. The influence of local sea surface temperatures on Australian east coast cyclones. *J. Geophys. Res. Atmos.,* doi: 10.1002/2016JD025495

Power, S. and Callaghan, J. 2016. The frequency of major flooding in coastal southeast Australia has significantly increased since the late 19th century. *Journal of Southern Hemisphere Earth Systems Science* 66:2–11, DOI: 10.22499/3.6601.002

PWD. 1985. Elevated coastal levels; Storms affecting N.S.W. coast 1880-1980. Report prepared by Blain, Bremner & Williams Pty Ltd in conjunction with Weatherex Meteorological Services Pty Ltd. Public Works Department. Report No 85041

Qi, L., Leslie, L. and Speer, M. 2006. Climatology of cyclones over the southwest Pacific: 1992–2001. Meteorol Atmos Phys 91, 201–209, doi:10.1007/s00703-005-0149-4.

Risbey, J.S., Pook, M.J., McIntosh, P.C., Wheeler, M.C. and Hendon, H.H. 2009. On the remote drivers of rainfall variability in Australia. Mon Wea Rev 137, 3233–3253, doi:10.1175/2009MWR2861.1

Risbey, J. S., Pook, M. J., McIntosh, P. C., Wheeler, M. C. and Hendon, H.H. 2009. On the Remote Drivers of Rainfall Variability in Australia, Mon. Weather Rev., 137, 3233–3253.

Simmonds, I., Murray, R.J. and Leighton, R.M. 1999. A refinement of cyclone tracking methods with data from FROST. *Aust. Meteorol. Mag.* (special edition): 35–49.

Speer, M.S., Wiles, P. and Pepler, A. 2009. Low pressure systems off the New South Wales coast and associated hazardous weather: establishment of a database Aust. Meteorol Oceanogr J 58, 29–39

Speer, M.S., Leslie, L.M. and Fierro, A.O. 2011. Australian east coast rainfall decline related to large scale climate drivers. Clim Dyn 36, 1419–1429, doi:10.1007/s00382-009-0726-1.

Trenberth, K.E**.** 1997. The Definition of El Niño. *Bulletin of the American Meteorological Society*, **78**, 2771-2777.

Uppala, S.P. and coauthors 2005. The ERA-40 re-analysis, *Quart. J. Roy. Meteor. Soc.*, 131, 2961–3012, doi:10.1256/qj.04.176.

Uppala, S.M., Dee, D.P., Kobayashi, S. and Simmons, A.J. 2008. 'Evolution of reanalysis at ECMWF'. In Proceedings of Third WCRP International Conference on Reanalysis, 28 January–1 February 2008, Tokyo, Japan.

Verdon-Kidd, D.C., Kiem, A.S., Willgoose, G. and Haines, P. 2010. East Coast Lows and the Newcastle/Central Coast Pasha Bulker storm. Report for the National Climate Change Adaptation Research Facility, Gold Coast, Australia.

Verdon-Kidd, D.C., Kiem, A.S. and Willgoose, G. 2016. East Coast Lows and the Pasha Bulker storm - lessons learned nine years on. Journal of Southern Hemisphere Earth Systems Science 66(2) 152-161

Wang, G. and Hendon, H.H. 2007: Sensitivity of Australian rainfall to inter-El Niño variations. Journal of Climate, 20, 4211-4226.

Wang, X.L., Feng, Y., Compo, G.P., Swail, V.R., Zwiers, F.W., Allan, R.J. and Sardeshmukh, P.D. 2013. Trends and low frequency variability of extra-tropical cyclone activity in the ensemble of twentieth century reanalysis. Clim. Dyn. 40: 2775–2800, doi: 10.1007/s00382-012-1450-9.

Table 1 Pearson's correlation (*r*) between ECL frequency and the major southern hemisphere climate mode indices for (a) annual and (b) winter (May to September). The time period of climate drivers is 1950-2014 for Nino3.4, 1951-2014 for SOI, 1957-2014 for SAM, 1870-2014 for IOD, and 1870-2015 for IPO and ENSO Modoki. The correlations are calculated for the overlap period from 1957-2014. The correlations for whole period are included in bracket for climate drivers with long record. The significant correlations at $p<0.05$ (according to a *t*-test) are highlighted.

(a) Annual ECLs	SOI	SAM	Nino3.4	Modoki(EMI)	IPO	IOD
LAP	0.20	0.08	-0.22	-0.08(-0.13)	-0.21 **(-0.28)**	**-0.39** (-0.14)
PG	**0.30**	0.02	**-0.33**	-0.18(-0.20)	**-0.31 (-0.31)**	**-0.27** (-0.02)
ULGV	0.15	-0.04	-0.14	0.03(-0.11)	-0.12 (-0.16)	**-0.37** (0.09)

(b) ECLs(May-Sept)	SOI	SAM	Nino3.4	Modoki(EMI)	IPO	IOD
LAP	**0.29**	0.04	-0.18	-0.05(-0.13)	-0.18(-0.19)	-0.21(-0.17)
PG	0.24	0.01	-0.18	-0.23(-0.21)	-0.19(-0.15)	-0.09(-0.07)
ULGV	**0.25**	0.12	-0.08	-0.05(-0.17)	-0.08(-0.11)	-0.08(0.05)

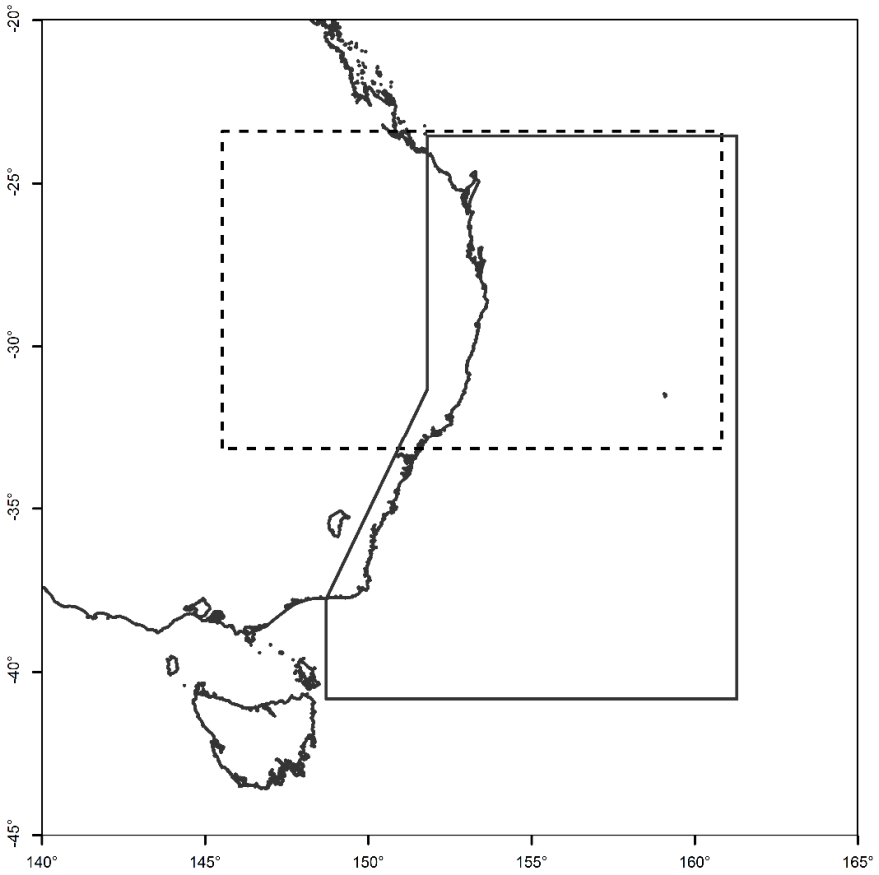

Figure 1. South-eastern Australia, with key features marked. The solid black lines indicate the domain for identifying ECLs in the surface pressure, while the dashed line indicates the corresponding region for detecting geostrophic vorticity maxima at 500 hPa (note the westward shift relative to the ECL domain).

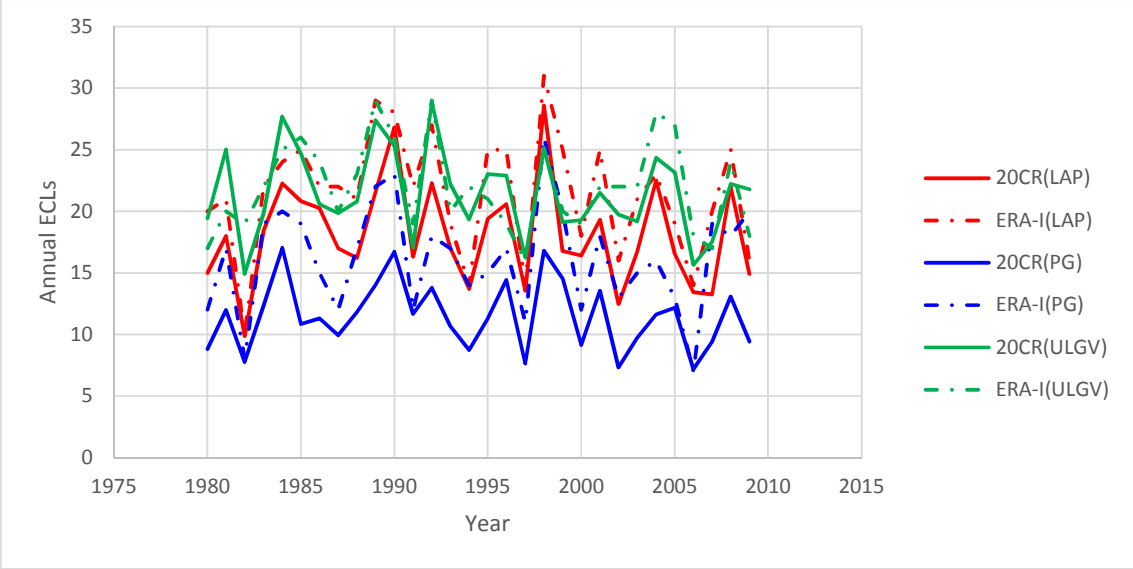

Figure 2. Annual ECL frequency tracked by three different methods for two reanalyses (20CR and ERA-I) Three colours are for three tracking methods, different line styles are for different reanalyses.

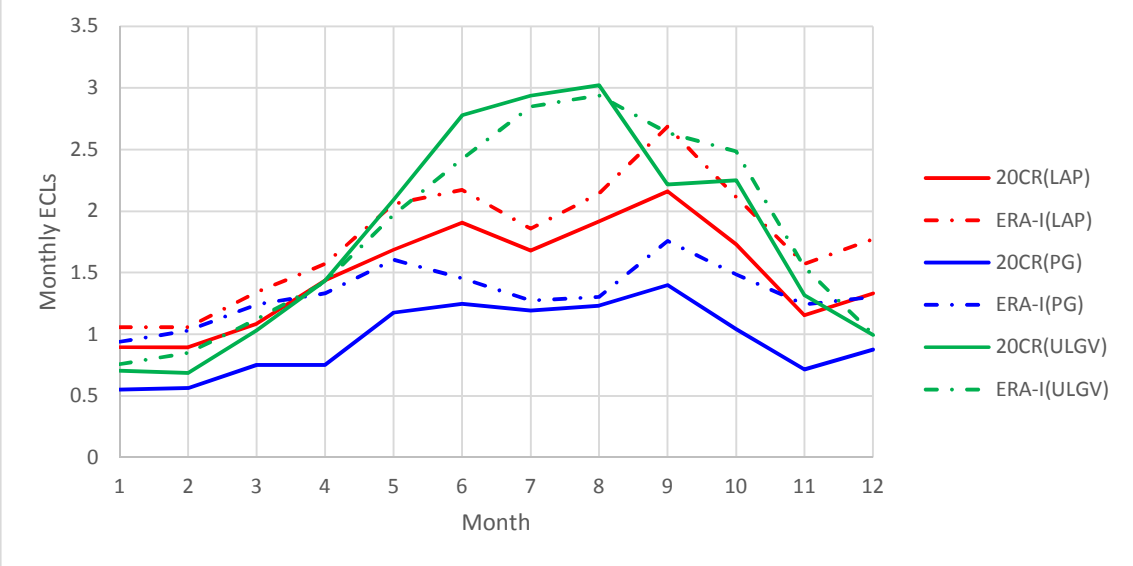

Figure 3. Distributions of monthly ECL frequency tracked by three different methods for two reanalyses (20CR and ERA-I) Three colours are for three tracking methods, different line styles are for different reanalyses.

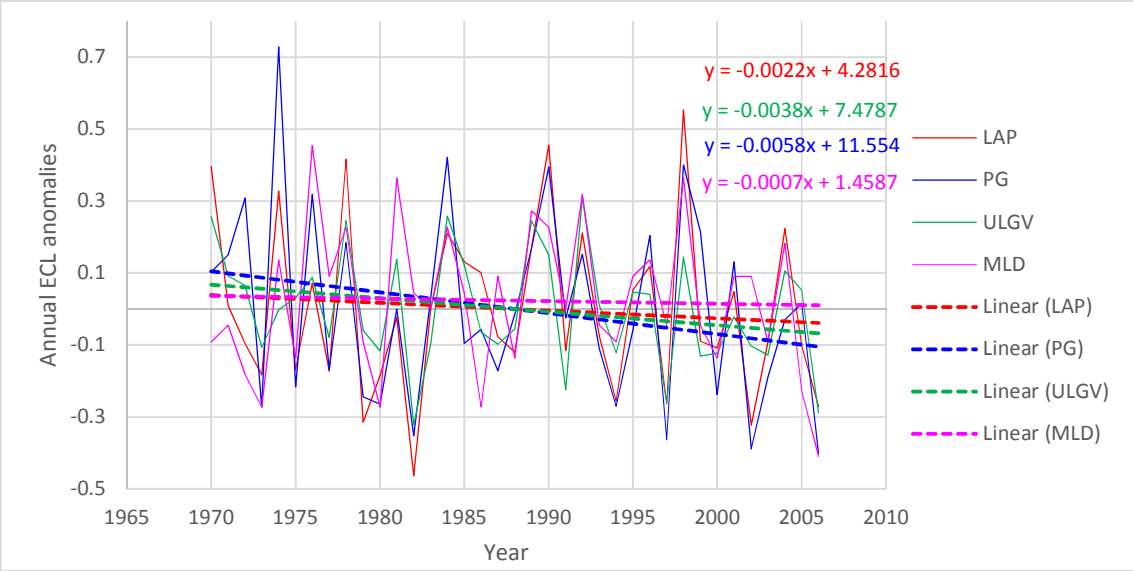

Figure 4 Normalized annual ECL frequency using three tracking methods and Maritime Low Database (MLD). The normalization is calculated against the mean number of ECLs for 1970-2006. The four different colours are for three tracking methods and MLD. The solid lines are for normalized annual ECLs and dot lines are trend lines for them.

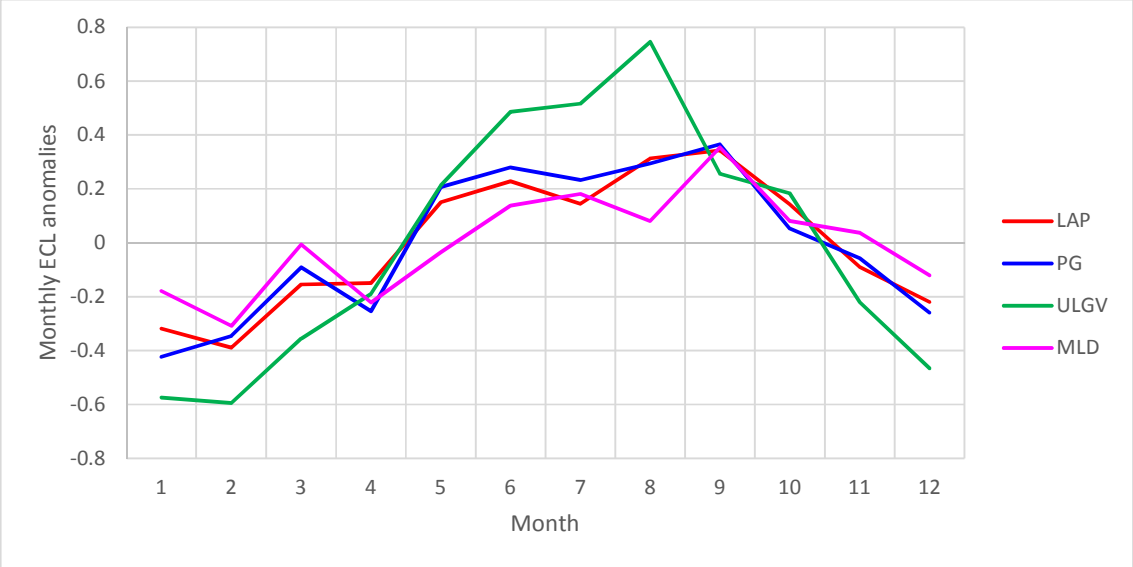

Figure 5. Normalized monthly ECL frequency for three tracking methods and MLD. The normalization is calculated against the mean number of monthly ECLs for 1970-2006. The four different colours are for three tracking methods and MLD.

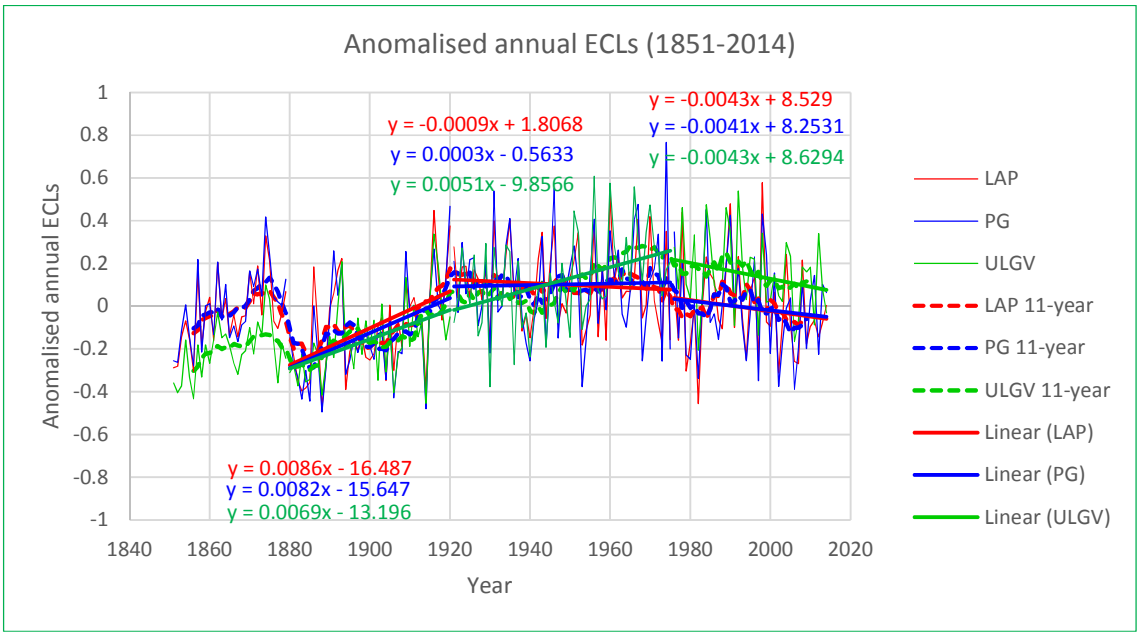

Figure 6 Normalized annual number of ECLs for three tracking methods. The normalization is calculated against the mean number of ECLs for 1970-2006. The three different colours are for three tracking methods, and thin solid lines are for annual ECL anomaly and dot lines are 11 year moving average, and solid lines are trend lines for 1880-1920, 1920-1975 and 1975 to 2014.

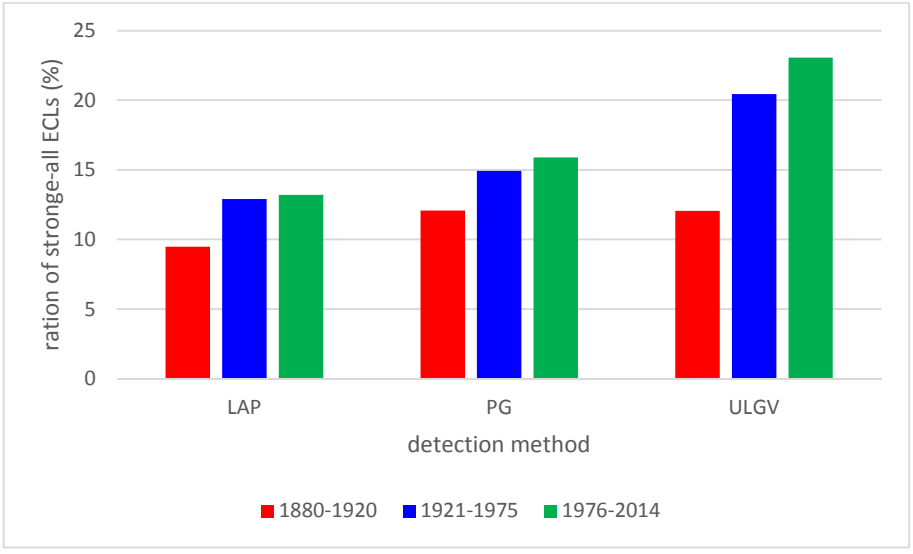

Figure 7 Ratio of strong ECLs for three time periods (1880-1920, 1920-1975 and 1975 to 2014) for three tracking methods

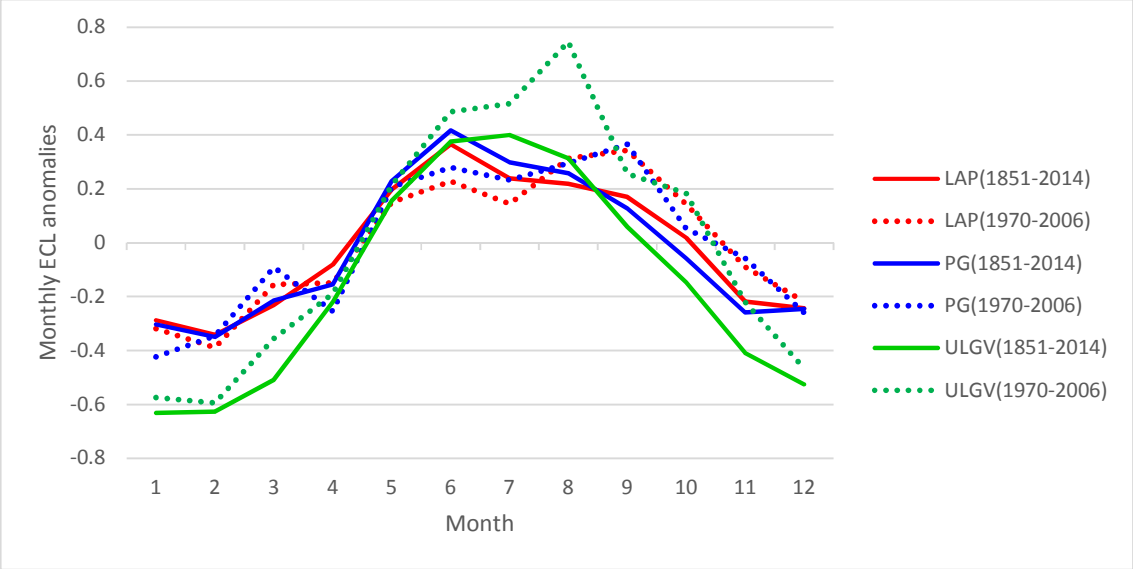

Figure 8 Normalized monthly ECLs for three tracking methods for 1851-2014 and 1970-2006. The normalization is calculated against the mean number of ECLs for 1970-2006. The three different colours are for three tracking methods, and solid lines are for 1851-2014 and dot lines are for 1970-2006.

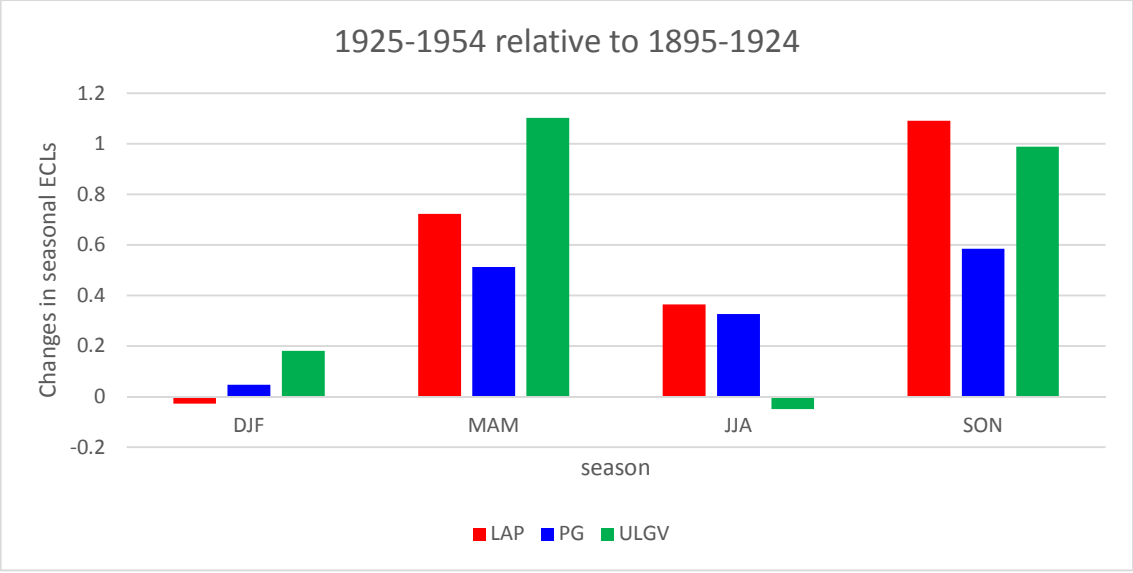

Figure 9 Changes in seasonal ECLs for two 30-year periods when the increasing trend is observed.

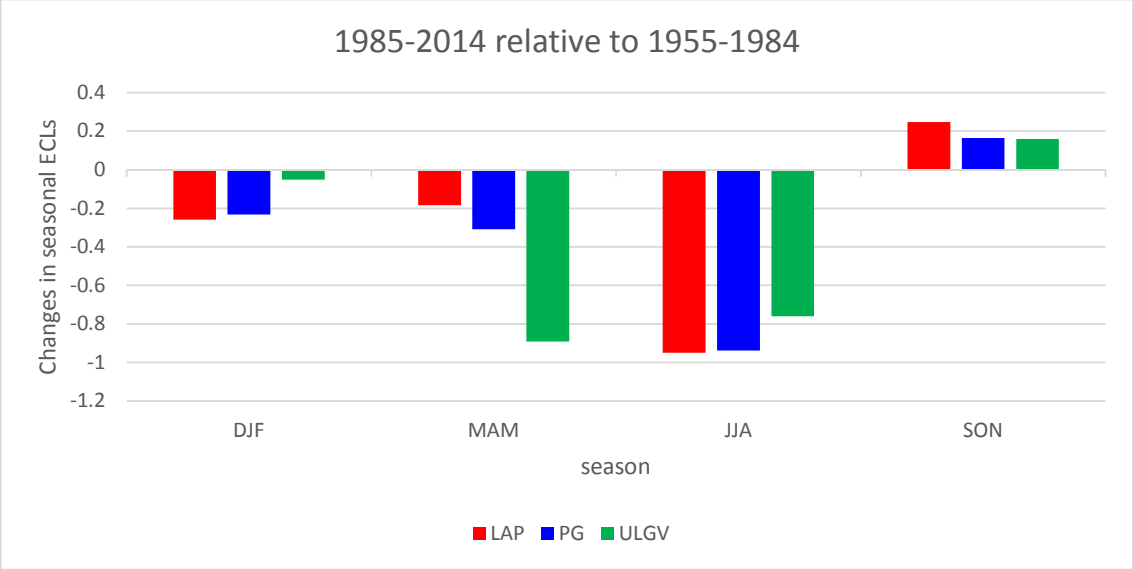

Figure 10 Changes in seasonal ECLs for two 30-year periods when the decreasing trend is observed

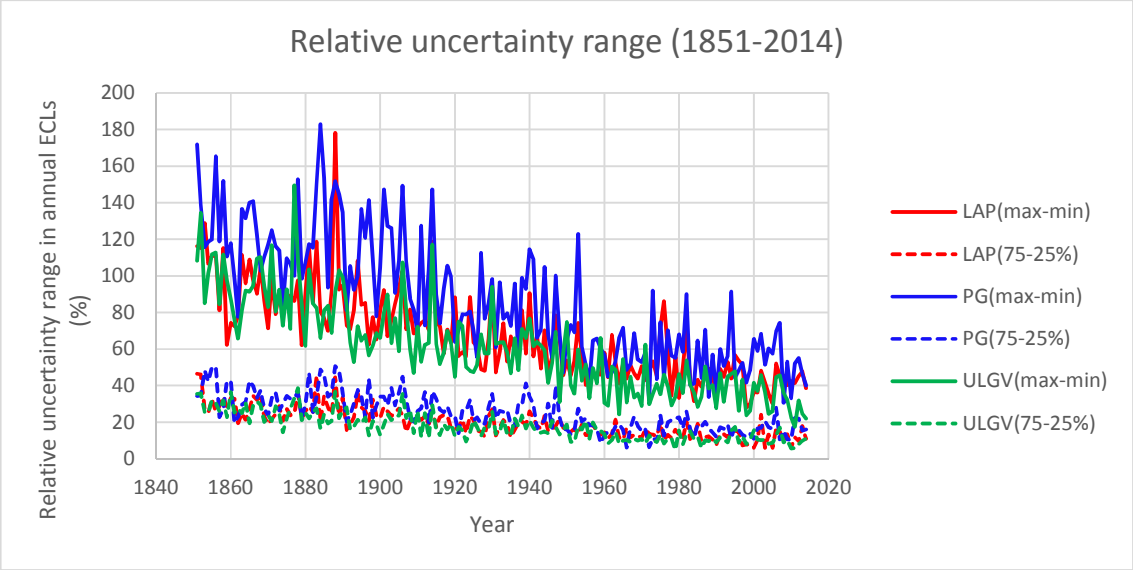

Figure 11 Relative uncertainty range of indicated annual ECLs for 1851-2014. Solid lines are for uncertainty between maximum and minimum number of identified ECLs of 56 ensemble members for three tracking methods. Dot lines are for uncertainty between 75 percentile and 25 percentile of identified ECLs of 56 ensemble members for three tracking methods.